Editors' Suggestion

Singlet/triplet Josephson junction on a substrate

Kaito Yamaki and Yasuhiro Asano
Department of Applied Physics, Hokkaido University, Sapporo 060-8628, Japan

(Received 3 April 2025; accepted 20 May 2025; published 4 June 2025)

We discuss the Josephson effect in a spin-singlet superconductor/spin-triplet superconductor junction fabricated on a substrate. Due to inversion symmetry breaking on top of the substrate, Rashba spin-orbit interaction works on electrons in the superconductors. As a result, spin-triplet (spin-singlet) Cooper pairs are induced in a spin-singlet (spin-triplet) superconductor. The presence of such induced Cooper pairs enables the lowest-order Josephson coupling between the two superconductors. Based on the theoretical results and recent experimental findings [X. Xu *et al.*, Phys. Rev. Lett. **132**, 056001 (2024)], we analyze the pair potential of β-Bi_2Pd.

DOI: 10.1103/PhysRevB.111.214505

I. INTRODUCTION

Symmetries of the pair potentials in superconductors are usually classified into either spin-singlet even-parity class or spin-triplet odd-parity class. Although spin-singlet superconductivity has been observed in various materials such as monoelement metals and high-T_c cuprates, spin-triplet superconductors (SCs) are very rare. The topological-material-based compound $Cu_xBi_2Se_3$ and several uranium compounds, such as UPt_3, UBe_{13}, UGe_2, and UTe_2, are candidates for spin-triplet SCs [1–7]. At present, however, spin-triplet superconductivity in these materials is still under debate. The search for spin-triplet SCs has been an important issue recently in order to realize quantum computation using non-Abelian statistics of Majorana fermions. In this situation, theoretical studies have proposed recipes for artificial spin-triplet SCs [8–11].

When a new candidate material is synthesized, several experiments are performed to confirm spin-triplet superconductivity. Critical magnetic fields beyond the Pauli limit and unchanged spin susceptibility across T_c are typical signatures of a spin-triplet SC. Experiments on normal-metal/superconductor (NS) proximity structures also tell us the signs for spin-triplet superconductivity, such as a zero-bias anomaly in the conductance spectra at a T-shaped junction [12,13] and unusual surface impedance in an NS bilayer [14]. These characteristic properties of a spin-triplet SC originate from a $\boldsymbol{d}$ vector (the order parameter of the spin-triplet superconductivity). In the ^{3}He B phase, for example, $\boldsymbol{d} \propto k_x\boldsymbol{e}_x + k_y\boldsymbol{e}_y + k_z\boldsymbol{e}_z$ is isotropic in both momentum and spin spaces, where $\boldsymbol{e}_j$, with $j = x, y$, and z, are the unit vector in spin space in the j direction. As a result, the spin susceptibility becomes isotropic in real space [15]. A $\boldsymbol{d}$ vector proportional to $(k_x + ik_y)$ breaks time-reversal symmetry and generates the intrinsic angular momentum in the ^{3}He A phase. Superconductivity in the heavy fermion compound UTe_2 may be described by a multicomponent $\boldsymbol{d}$ vector breaking time-reversal symmetry [16]. Thus, analyzing $\boldsymbol{d}$ in a spin-triplet SC is the most important issue in experimental research. In particular, the observation of the π-phase shift in a superconducting quantum interference device (SQUID) proposed by Geshkenbein, Larkin, and Barone (GLB) convincingly suggests spin-triplet superconductivity [17]. Indeed, based on the observed π-phase shift, a recent experiment [18] indicated spin-triplet superconductivity in a topologically nontrivial SC β-Bi_2Pd [19–21].

In a spin-singlet superconductor/spin-triplet superconductor junction (referred to as a singlet/triplet junction below), the lowest-order coupling is absent due to the mismatch of the pair potentials in spin space. Namely, spin-dependent potentials are necessary to have the lowest-order Josephson coupling in a singlet/triplet junction. Unfortunately, GLB did not discuss how symmetry mismatches are resolved in realistic junctions. Spin-orbit interaction (SOI) at the junction interface [22] is a possible source that enables the lowest-order coupling in a singlet/triplet junction. However, as we will show in Sec. V, the interface SOI does not explain the π-phase shift in a SQUID.

In this paper, we study the effects of the Rashba SOI on the Josephson current in a singlet/triplet junction fabricated on a substrate. The Rashba SOI generates a spin-triplet pairing correlation in a spin-singlet superconductor and spin-singlet pairing correlations in a spin-triplet superconductor. Such induced pairing correlations cause the lowest-order coupling in a singlet/triplet junction. In addition, the π-phase shift observed in a SQUID can be explained consistently by the selection rules derived from the Rashba SOI. We discuss the symmetry of the pair potential in β-Bi_2Pd while taking the selection rules into account.

This paper is organized as follows. We explain our theoretical model in Sec. II. The analytical expression for the Josephson current is presented in Sec. III. The selection rules for the Josephson coupling are discussed in Sec. IV. We analyze the pairing symmetry in β-Bi_2Pd in Sec. V. The conclusion is given in Sec. VI. We use units of $k_B = \hbar = c = 1$, where k_B is the Boltzmann constant and c is the speed of light.

II. MODEL

Let us consider a singlet/triplet Josephson junction, as shown in Fig. 1. Two superconducting thin films are fabricated on a substrate and form a Josephson junction at $x = 0$.

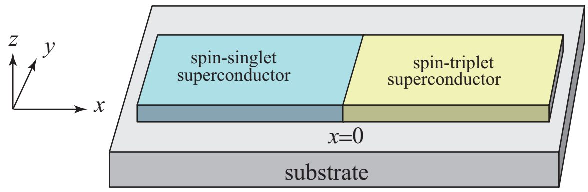

FIG. 1. Schematic picture of a spin-singlet superconductor/spin-triplet superconductor junction, referred to as a singlet/triplet junction in this paper. The current flows in the x direction, and the junction interface is at $x = 0$. The cross section of the junction is S.

The normal state Hamiltonian in a uniform superconductor is given by

$$\hat{H}_{\rm N}(j,\boldsymbol{k}) = \xi_{j,\boldsymbol{k}} - \boldsymbol{\alpha}_{\boldsymbol{k}} \cdot \hat{\boldsymbol{\sigma}}, \tag{1}$$

$$\boldsymbol{\alpha}_{\boldsymbol{k}} = (-\lambda k_y, \lambda k_x, 0), \tag{2}$$

$$\xi_{j,\boldsymbol{k}} = \frac{\boldsymbol{k}^2}{2m_j} + \epsilon_j - \mu, \tag{3}$$

where μ is the chemical potential and $\hat{\sigma}_i$ ($i = x, y,$ and z) is the Paul matrices in spin space. The effective mass of an electron and the energy shift are the material parameters. They are given by $m_j = m_s$ and $\epsilon_j = \epsilon_s$ in a singlet SC and $m_j = m_t$ and $\epsilon_j = \epsilon_t$ in a triplet SC. As inversion symmetry is broken along the z direction, Rashba SOI acts on electrons in thin SCs on a substrate. The pair potential in a spin-singlet SC is described as

$$\hat{\Delta}(s,\boldsymbol{k}) = \Delta_{\boldsymbol{k}}\, i\hat{\sigma}_y\, e^{i\varphi_s}, \quad \Delta_{-\boldsymbol{k}} = \Delta_{\boldsymbol{k}}, \tag{4}$$

where φ_s is the phase of the superconducting condensate. The pair potential in a spin-triplet SC is given by

$$\hat{\Delta}(t,\boldsymbol{k}) = i\boldsymbol{d}_{\boldsymbol{k}} \cdot \hat{\boldsymbol{\sigma}}\, \hat{\sigma}_y\, e^{i\varphi_t}, \quad \boldsymbol{d}_{-\boldsymbol{k}} = -\boldsymbol{d}_{\boldsymbol{k}}, \tag{5}$$

where φ_t is the phase and the three-component vector $\boldsymbol{d}_{\boldsymbol{k}}$ describes spin-triplet superconductivity. Throughout this paper, we consider unitary states (i.e., $\boldsymbol{d}_{\boldsymbol{k}} \times \boldsymbol{d}^*_{\boldsymbol{k}} = 0$).

The Hamiltonian in each superconductor is described by

$$\mathcal{H}_j = \sum_{\boldsymbol{k}} \Psi^\dagger_j(\boldsymbol{k})\, H_j(\boldsymbol{k})\, \Psi_j(\boldsymbol{k}), \tag{6}$$

$$H_j(\boldsymbol{k}) = \begin{bmatrix} \hat{H}_{\rm N}(j,\boldsymbol{k}) & \hat{\Delta}(j,\boldsymbol{k}) \\ -\underset{\sim}{\hat{\Delta}}(j,\boldsymbol{k}) & -\underset{\sim}{\hat{H}}_{\rm N}(j,\boldsymbol{k}) \end{bmatrix}, \tag{7}$$

$$\Psi_j(\boldsymbol{k}) = [c_{j,\boldsymbol{k},\uparrow}, c_{j,\boldsymbol{k},\downarrow}, c^\dagger_{j,-\boldsymbol{k},\uparrow}, c^\dagger_{j,-\boldsymbol{k},\downarrow}]^{\rm T} \tag{8}$$

for $j = s$ and t, where $c_{j,\boldsymbol{k},\sigma}$ is the annihilation operator of an electron with a wave number $\boldsymbol{k}$ and spin σ in a SC labeled by j. Particle-hole conjugation is denoted by $\underset{\sim}{X}(\boldsymbol{k},\omega_n) \equiv X^*(-\boldsymbol{k},\omega_n)$. The Green's function in each SC is calculated as a solution of the Gor'kov equation,

$$[i\omega_n - H_j(\boldsymbol{k})] \begin{bmatrix} \hat{G}_j(\boldsymbol{k},\omega_n) & \hat{F}_j(\boldsymbol{k},\omega_n) \\ -\underset{\sim}{\hat{F}}_j(\boldsymbol{k},\omega_n) & -\underset{\sim}{\hat{G}}_j(\boldsymbol{k},\omega_n) \end{bmatrix} = 1_{4\times 4}, \tag{9}$$

where $\omega_n = (2n+1)\pi T$ is the fermionic Matsubara frequency, with T being a temperature. The coupling between the two SCs is described phenomenologically by a tunnel Hamiltonian,

$$\mathcal{H}_T = \sum_{\boldsymbol{k},\boldsymbol{p},\sigma} [-t_{\boldsymbol{k},\boldsymbol{p}}\, c^\dagger_{t,\boldsymbol{k},\sigma}\, c_{s,\boldsymbol{p},\sigma} - t_{\boldsymbol{k},\boldsymbol{p}}\, c^\dagger_{s,\boldsymbol{p},\sigma}\, c_{t,\boldsymbol{k},\sigma}]. \tag{10}$$

Within the linear response, the Josephson current between the two SCs is calculated as [23]

$$J = -2eT \sum_{\omega_n} \sum_{\boldsymbol{k},\boldsymbol{p}} {\rm Im\,Tr}[t_{\boldsymbol{k},\boldsymbol{p}}\, \hat{F}_s(\boldsymbol{p})\, t_{-\boldsymbol{k},-\boldsymbol{p}}\, \underset{\sim}{\hat{F}_t}(\boldsymbol{k})]. \tag{11}$$

III. CURRENT

The anomalous Green's function is calculated as

$$\hat{F}_s(\boldsymbol{k},\omega_n) = -\frac{\left(\omega_n^2 + \xi^2_{s,\boldsymbol{k}} + |\Delta_{\boldsymbol{k}}|^2 + \boldsymbol{\alpha}^2_{\boldsymbol{k}}\right) + 2\xi_{s,\boldsymbol{k}}\boldsymbol{\alpha}_{\boldsymbol{k}} \cdot \hat{\boldsymbol{\sigma}}}{Z_s} \times \Delta_{\boldsymbol{k}}\, i\hat{\sigma}_y\, e^{i\varphi_s}, \tag{12}$$

$$Z_s = \left(\omega_n^2 + \xi^2_{s,\boldsymbol{k}} + |\Delta_{\boldsymbol{k}}|^2 + \boldsymbol{\alpha}^2_{\boldsymbol{k}}\right)^2 - 4\xi^2_{s,\boldsymbol{k}}\, \boldsymbol{\alpha}^2_{\boldsymbol{k}}, \tag{13}$$

in a spin-singlet SC. The first four terms in the numerator of Eq. (12) represent a spin-singlet pairing correlation that is linked to the pair potential through the gap equation in the presence of an attractive interaction between two electrons. The last term describes a spin-triplet odd-parity pairing correlation induced by the SOI. The results in a spin-triplet SC are given by

$$\begin{aligned} \hat{F}_t(\boldsymbol{k},\omega_n) = &-\frac{1}{Z_t}\Big[\left(\omega_n^2 + \xi^2_{s,\boldsymbol{k}} + |\boldsymbol{d}_{\boldsymbol{k}}|^2 - \boldsymbol{\alpha}^2_{\boldsymbol{k}}\right)\boldsymbol{d}_{\boldsymbol{k}} \cdot \hat{\boldsymbol{\sigma}} \\ &+ 2(\boldsymbol{\alpha}_{\boldsymbol{k}} \cdot \boldsymbol{d}_{\boldsymbol{k}})\boldsymbol{\alpha}_{\boldsymbol{k}} \cdot \hat{\boldsymbol{\sigma}} + 2\omega_n(\alpha_{\boldsymbol{k}} \times \boldsymbol{d}_{\boldsymbol{k}}) \cdot \hat{\boldsymbol{\sigma}} \\ &- 2\xi_{t,\boldsymbol{k}}\, \boldsymbol{\alpha}_{\boldsymbol{k}} \cdot \boldsymbol{d}_{\boldsymbol{k}}\Big]\, i\,\hat{\sigma}_y\, e^{i\varphi_t}, \end{aligned} \tag{14}$$

$$\begin{aligned} Z_t = &\left(\omega_n^2 + \xi^2_{t,\boldsymbol{k}} + |\boldsymbol{d}_{\boldsymbol{k}}|^2 + \boldsymbol{\alpha}^2_{\boldsymbol{k}}\right)^2 - 4\xi^2_{t,\boldsymbol{k}}\, \boldsymbol{\alpha}^2_{\boldsymbol{k}} \\ &- 4|\boldsymbol{\alpha}_{\boldsymbol{k}} \times \boldsymbol{d}_{\boldsymbol{k}}|^2. \end{aligned} \tag{15}$$

The first line of Eq. (14) represents a spin-triplet pairing correlation linked to the pair potential. The SOI generates three extra pairing correlations. The first term in the second line describes such a spin-triplet odd-parity pairing correlation. The pairing correlation in the second term in the second line belongs to the odd-frequency spin-triplet even-parity symmetry class. The last term describes a spin-singlet even-parity pairing correlation. The spin-singlet and spin-triplet mixed states are realized in the two SCs, which enables the lowest-order Josephson coupling between them.

At low temperatures, the tunnel Hamiltonian (10) works only on electrons at the Fermi level. The wave number in the current direction is limited to

$$\frac{p_x^2 + \boldsymbol{p}_\parallel^2}{2m_s} + \epsilon_s - \mu = 0, \quad \frac{k_x^2 + \boldsymbol{k}_\parallel^2}{2m_t} + \epsilon_t - \mu = 0, \tag{16}$$

where $\boldsymbol{p}_\parallel(\boldsymbol{k}_\parallel)$ is the wave number in the yz plane on the Fermi surface at a singlet (triplet) SC. The Fermi wave number is defined as $k_{F,j} = \sqrt{2m_j(\mu - \epsilon_j)}$ for $j = s$ and t. As a result of translational symmetry in the yz plane, the wave number in the directions parallel to the plane is preserved in the tunnel process,

$$\boldsymbol{p}_\parallel = \boldsymbol{k}_\parallel. \tag{17}$$

Namely, the tunneling event happens between the states on the Fermi surface at $(\pm p_x, \boldsymbol{k}_\parallel)$ in a spin-singlet SC and those at $(\pm k_x, \boldsymbol{k}_\parallel)$ in a spin-triplet SC. In what follows, we assume that the tunneling amplitude is a constant independent of wave number, (i.e., $t_{\boldsymbol{k},\boldsymbol{p}} = t\,\delta_{\boldsymbol{k}_\parallel,\boldsymbol{p}_\parallel}$). The summation over the wave number is expressed as

$$\sum_{\boldsymbol{k}} F(\xi_{\boldsymbol{k}}, \hat{\Delta}_{\boldsymbol{k}}) \to \int d\xi_j N(\xi_j) \langle F(\xi_j, \hat{\Delta}_{\boldsymbol{k}})\rangle_{\bar{\boldsymbol{k}}_\parallel}, \tag{18}$$

$$\langle F(\xi_j, \hat{\Delta}_{\boldsymbol{k}})\rangle_{\bar{\boldsymbol{k}}_\parallel} = \frac{1}{\pi}\int_0^\pi d\theta \sin^2\theta \int_{-\pi/2}^{\pi/2} d\phi \cos\phi \times F(\xi_j, \hat{\Delta}_{k_x,\boldsymbol{k}_\parallel}), \tag{19}$$

where $N(\xi_j)$ is the density of states per spin. The wave number on the Fermi surface is parameterized as $k_x = k_{F,j}\sin\theta\,\cos\phi$, $k_y = k_{F,j}\sin\theta\,\sin\phi$, and $k_z = k_{F,j}\cos\theta$. $\langle\cdots\rangle$ in Eq. (19) means summation over the propagating channels on the Fermi surface with $k_x > 0$, where $\boldsymbol{k}_\parallel = k_y\bar{\boldsymbol{y}} + k_z\bar{\boldsymbol{z}}$, $\bar{\boldsymbol{k}}_\parallel = \boldsymbol{k}_\parallel/k_{F,j}$, and $\bar{\boldsymbol{y}}$ ($\bar{\boldsymbol{z}}$) is the unit vector in the y (z) direction.

The Josephson current is expressed as

$$J = \frac{\pi}{eR_{\rm N}} T \sum_{\omega_n} {\rm Im}\left\langle \frac{e^{i\varphi}\,\delta_{\boldsymbol{k}_\parallel,\boldsymbol{p}_\parallel}(X_t - X_s)\Delta_{\boldsymbol{p}}}{\sqrt{\omega_n^2 + |\Delta_{\boldsymbol{p}}|^2}\sqrt{\omega_n^2 + |\boldsymbol{d}_{\boldsymbol{k}}|^2}} \frac{\boldsymbol{\alpha}_{\boldsymbol{k}}\cdot\boldsymbol{d}^*_{\boldsymbol{k}}}{|\boldsymbol{\alpha}_{\boldsymbol{k}}|} \right\rangle_{\bar{\boldsymbol{k}}_\parallel}, \tag{20}$$

with

$$R_{\rm N}^{-1} = 4\pi e^2 t^2 N_s(0) N_t(0), \quad \varphi = \varphi_s - \varphi_t, \tag{21}$$

$$X_j = \frac{|\boldsymbol{\alpha}_{\boldsymbol{k}}|}{N_j(0)} \left.\frac{dN_j(\xi_j)}{d\xi_j}\right|_{\xi_j=0} \approx \frac{\lambda k_{F,j}}{\mu - \epsilon_j} \ll 1 \tag{22}$$

for $j = s$ and t, where $R_{\rm N}$ is the resistance of the junction in the normal state. In Appendix A, we discuss how to derive Eq. (20). Equation (20) represents the Josephson current due to the coupling between the pair potential and the pairing correlations induced by Rashba SOI. As the induced spin-triplet component in Eq. (12) is proportional to ξ_s, the Josephson current due to such coupling is proportional to X_s in Eq. (20). The energy derivative of the density of states determines the amplitude of the Josephson current. In a similar way, the coupling between the induced spin-singlet correlation in a spin-triplet SC and the spin-singlet pair potential $\Delta_{\boldsymbol{p}}$ carries a Josephson current proportional to X_t in Eq. (20). The amplitude of the Josephson current at zero temperature is roughly estimated as $X_j J_0$, where J_0 in Eq. (A8) is the amplitude of the critical current in the Ambegaokar-Baratoff formula [24].

The results in Eq. (20) also tell us the current-phase relationship (CPR). When both $\Delta_{\boldsymbol{k}}$ and $\boldsymbol{d}_{\boldsymbol{k}}$ are real numbers, the CPR is sinusoidal because $J \propto \sin\varphi$. For chiral states such as the chiral d-wave $\Delta_{\boldsymbol{k}} \propto (k_x + ik_y)k_z$ and the chiral p-wave $\boldsymbol{d}_{\boldsymbol{k}} \propto k_x + ik_y$, the CPR may deviate from the sinusoidal function.

IV. SELECTION RULES

A singlet/triplet junction is usually used as a symmetry tester for a spin-triplet SC. Therefore, conventional superconductors such as Nb, Al, and Pb are adopted at a spin-singlet segment. The Josephson current in such a junction becomes

$$J = J_0\frac{2\Delta}{\Delta_0} T \sum_{\omega_n} {\rm Im}\, e^{i\varphi}\frac{X_t - X_s}{\sqrt{\omega_n^2 + \Delta^2}} \times \left\langle \frac{1}{\sqrt{\omega_n^2 + |\boldsymbol{d}_{\boldsymbol{k}}|^2}} \frac{k_y\, d_x^*(\boldsymbol{k}) - k_x\, d_y^*(\boldsymbol{k})}{\sqrt{k_x^2 + k_y^2}} \right\rangle_{\bar{\boldsymbol{k}}_\parallel}. \tag{23}$$

The results imply the selection rules for two parts of $\boldsymbol{d}_{\boldsymbol{k}}$: the spin part and the orbital part. The Rashba SOI does not couple to the z component of $\boldsymbol{d}_{\boldsymbol{k}}$ that represents a spin-triplet Cooper pair with its spin polarizing in the xy plane. The selection rules for the orbital part are derived from the average over $\boldsymbol{k}_\parallel = k_y\bar{\boldsymbol{y}} + k_z\bar{\boldsymbol{z}}$. The x component of $\boldsymbol{d}_{\boldsymbol{k}}$ must be an odd function of k_y for the average in Eq. (23) to be a nonzero value. In the same manner, d_y must be an even function of $\boldsymbol{k}_\parallel$ for a finite Josephson coupling under the odd-parity condition $\boldsymbol{d}_{\boldsymbol{k}} = -\boldsymbol{d}_{-\boldsymbol{k}}$. The selection rules due to Rashba SOI are summarized in the first column in Table I.

TABLE I. The selection rules for $\boldsymbol{d}_{\boldsymbol{k}}$ are summarized for the lowest-order Josephson coupling. For the Rashba SOI, the Josephson current flows when $\boldsymbol{d}_{\boldsymbol{k}}$ has a component of $d_x \propto k_y$, as indicated in the first row, and/or $d_y \propto k_x$, as indicated in the second row. In the first row, the presence of $d_x \propto k_y$ gives the interference pattern in Fig. 2(a), as shown by circles (○). But it does not explain the interference pattern in Fig. 2(b), as shown by crosses (×). In the second row, the presence of $d_y \propto k_x$ successfully explains both interference patterns in Fig. 2. The Rashba SOI does not couple to the z component of $\boldsymbol{d}_{\boldsymbol{k}}$. The selection rules due to the interface SOI in Eq. (24) [22] are also shown. The interface SOI cannot give the Josephson coupling that reproduces the interference pattern in Fig. 2(b).

Pair potential	Fig. 2(a)	Fig. 2(b)
Rashba SOI		
$d_x(\boldsymbol{k}) \propto k_y$	○	×
$d_y(\boldsymbol{k}) \propto k_x$	○	○
$d_z(\boldsymbol{k})$ no coupling	×	×
Interface SOI $\boldsymbol{j} \parallel \boldsymbol{x}$		
$d_x(\boldsymbol{k})$ no coupling		×
$d_y(\boldsymbol{k}) \propto k_z$		×
$d_z(\boldsymbol{k}) \propto k_y$		×
Interface SOI $\boldsymbol{j} \parallel \boldsymbol{y}$		
$d_x(\boldsymbol{k}) \propto k_z$	○	
$d_y(\boldsymbol{k})$ no coupling	×	
$d_z(\boldsymbol{k}) \propto k_x$	○	

For comparison, we briefly derive the selection rules due to SOI at the junction interface proposed by Millis *et al.* [22]. The SOI originates from breaking inversion symmetry in the x direction at the junction interface. Therefore, electronic structures in the two SCs must be different from each other [25] (i.e., $m_s \neq m_t$ and/or $\epsilon_s \neq \epsilon_t$). The interface SOI is described by

$$H_I = \lambda_I(\nabla V(\boldsymbol{r})) \times \hat{\boldsymbol{\sigma}}\cdot\boldsymbol{k}, \tag{24}$$

where $V(\boldsymbol{r})$ is the potential barrier at the interface. For the current flowing in the x direction, the Josephson current with

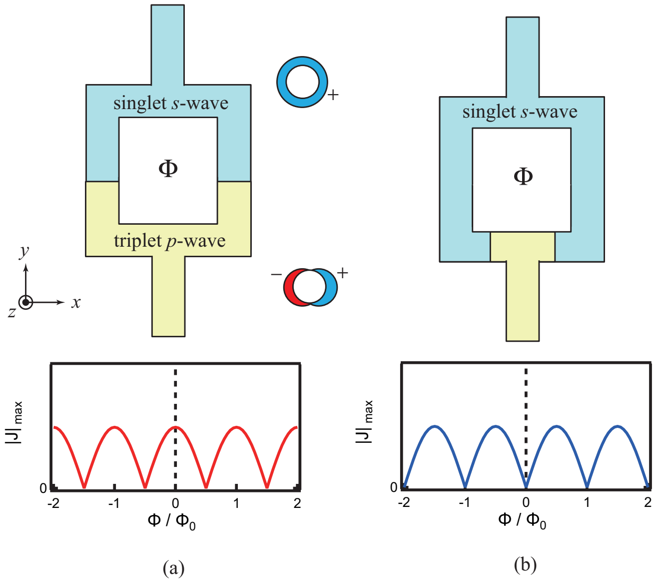

FIG. 2. Schematic picture of two SQUIDs and expected interference patterns. We consider a conventional s-wave pair potential in a spin-singlet superconductor. The interference pattern in (b) is observed only when $\boldsymbol{d_k}$ has a component proportional to k_x and the component forms the Josephson coupling. The images of the pair potentials are also illustrated on a two-dimensional Fermi surface.

$\nabla V(\boldsymbol{r}) \parallel \boldsymbol{x}$ and $\boldsymbol{k}_\parallel = k_y\bar{\boldsymbol{y}} + k_z\bar{\boldsymbol{z}}$ is represented as

$$J_I^{(x)} \propto \langle k_z\, d_y^*(\boldsymbol{k}) - k_y\, d_z^*(\boldsymbol{k})\rangle_{\bar{\boldsymbol{k}}_\parallel}. \tag{25}$$

To have a nonzero Josephson coupling, d_y must be proportional to k_z, and/or d_z must be proportional to k_y. The x component of $\boldsymbol{d_k}$ does not contribute to the Josephson current. The results are summarized for the interface SOI $\boldsymbol{j} \parallel \boldsymbol{x}$ in Table I.

The selection rules for the interface SOI depends on the current direction. For the current in the y direction the Josephson current with $\nabla V(\boldsymbol{r}) \parallel \boldsymbol{y}$ and $\boldsymbol{k}_\parallel = k_x\bar{\boldsymbol{x}} + k_z\bar{\boldsymbol{z}}$ is calculated as

$$J_I^{(y)} \propto \langle k_z\, d_x^*(\boldsymbol{k}) - k_x\, d_z^*(\boldsymbol{k})\rangle_{\bar{\boldsymbol{k}}_\parallel}. \tag{26}$$

The y component of $\boldsymbol{d_k}$ does not contribute to the Josephson current. The relations $d_x \propto k_z$ and/or $d_z \propto k_x$ are necessary for the lowest-order Josephson coupling. Equation (24) indicates that the Josephson current due to the interface SOI for the current in the l direction can be described as

$$J^{(l)} \propto \langle \epsilon_{l,m,n}\, d_m\, k_n\rangle_{\bar{\boldsymbol{k}}_\parallel}, \quad \boldsymbol{k}_\parallel = k_n\bar{\boldsymbol{n}} + k_m\bar{\boldsymbol{m}}, \tag{27}$$

where $\epsilon_{l,m,n}$ are the antisymmetric tensors. Therefore, $\boldsymbol{d_k}$ proportional to k_l do not contribute to the Josephson coupling.

V. EXPERIMENT IN TWO SQUIDS

A previous paper [17] proposed a phase-sensitive experiment to identify a spin-triplet odd-parity SC using two SQUIDs as shown in Fig. 2, where Φ is the magnetic flux through the hole and $\Phi_0 = \pi/e$. When superconducting states are uniform, the two singlet/triplet junctions in Fig. 2(a) are identical to each other irrespective of symmetries in the pair potential. The maximum value of the Josephson current $|J_{\max}|$ takes its maximum at $\Phi = 0$, as shown in the bottom panel of Fig. 2(a). Details of the derivation are given in Appendix B, where we assume that the two junctions are zero junctions at $\Phi = 0$ and the CPR is sinusoidal, $J = J_{\rm ST} \sin\varphi$. In the SQUID in Fig. 2(b), the two singlet/triplet junctions are not identical to each other when $\boldsymbol{d_k}$ has an odd-parity component proportional to k_x. When one junction is a zero junction, the other becomes a π junction. As a result, $|J_{\max}|$ takes its minimum at $\Phi = 0$, as shown in the bottom panel of Fig. 2(b). Thus, the difference between the two interference patterns in Fig. 2 could be direct evidence of spin-triplet odd-parity superconductivity. In particular, the interference pattern in Fig. 2(b) is an essential property of spin-triplet SCs. In this section, we refine these phenomenological arguments by taking into account the selection rules in Table I.

We first discuss the selection rules for the interface SOIs. For the SQUID in Fig. 2(a) with the current in the y direction, the interference pattern in Fig. 2(a) can be explained when $\boldsymbol{d_k}$ has components of $d_x \propto k_z$ and/or $d_z \propto k_x$. In the second column in Table I, a circle means that the presence of such components reproduces the interference pattern in Fig. 2(a). Generally speaking, any lowest-order singlet/triplet couplings result in the interference pattern in Fig. 2(a). On the other hand, to explain the interference pattern in Fig. 2(b), the SOI is necessary to couple to a component of $\boldsymbol{d_k}$ proportional to k_x. The selection rules for the interface SOI with $\boldsymbol{j} \parallel \boldsymbol{x}$ are presented in Table I. In the last column, a cross means that the Josephson coupling due to the interface SOI cannot give the interference pattern in Fig. 2(b). This conclusion is independent of the details of $\boldsymbol{d_k}$. Therefore, the phenomenological theory by GLB [17] requires mechanisms of the singlet/triplet coupling other than the interface SOI.

Second, we examine the possibility of the Rashba SOI. The selection rules discussed with Eq. (23) can be applied to the SQUID in Fig. 2(b) because the current flows in the x direction. The Rashba SOI couples to two components: $d_x \propto k_y$ and $d_y \propto k_x$. In the former case, both singlet/triplet junctions in Fig. 2(b) become zero junctions or π junctions simultaneously because $d_x \propto k_y$ is an even function of k_x. Thus, such coupling cannot explain the interference pattern in Fig. 2(b), as indicated by a cross in the last column in Table I. On the other hand, the latter case, $d_y \propto k_x$, is an odd function of k_x. As a result, one singlet/triplet junction in Fig. 2(b) becomes a π junction, and the other becomes a zero junction, which explains the interference pattern in Fig. 2(b), as indicated by circles in Table I. The results for the SQUID in Fig. 2(a) are derived by considering $\boldsymbol{k}_\parallel = k_x\bar{\boldsymbol{x}} + k_z\bar{\boldsymbol{z}}$ because the current flows in the y direction. It is easy to confirm that the first column in Table I remains unchanged and both $d_x \propto k_y$ and $d_y \propto k_x$ give the interference pattern in Fig. 2(a). Thus, the Rashba SOI generates the single/triplet Josephson coupling necessary for the SQUID in Fig. 2(b) to function as a symmetry testing device [17]. The experimental findings [18] strongly suggest that $\boldsymbol{d_k}$ in β-Bi_2Pd must have a component of $d_y \propto k_x$. As briefly mentioned in the Introduction, the characteristic properties of a spin-triplet SC originate from its $\boldsymbol{d}$ vector. The component of $d_y \propto k_x$ can be confirmed by an another junction experiment, in which a spin-singlet SC is replaced by a normal metal in Fig. 1. The conclusion, $d_y \propto k_x$, suggests that the anomalous proximity effect is expected in

TABLE II. Symmetry classification of the pair potentials for multiband/orbital superconductors.

Spin	Momentum parity	Band parity
Singlet	Even	Even
Triplet	Odd	Even
Singlet	Odd	Odd
Triplet	Even	Odd

the normal metal and that this effect can be confirmed by the conductance spectroscopy in a T-shaped junction [12,13].

Third, we briefly discuss the effects of SOIs in a bulk spin-triplet SC derived from lattice structures such as Rashba SOI in noncentrosymmetric SCs and Dresselhaus SOI. These SOIs can be a source of anisotropy in the magnetic susceptibility in both normal and superconducting states. The current expression in Eq. (20) can be applied to any triplet SCs $\boldsymbol{d}_{\boldsymbol{k}}$ and to any SOIs $\boldsymbol{\alpha}_{\boldsymbol{k}}$. As displayed in Eq. (14), $\langle \boldsymbol{\alpha}_{\boldsymbol{k}} \cdot \boldsymbol{d}_{\boldsymbol{k}} \rangle_{\bar{k}_\parallel} \neq 0$ is a necessary condition for the lowest-order Josephson coupling in Fig. 2(b). Therefore, the product $\boldsymbol{\alpha}_{\boldsymbol{k}} \cdot \boldsymbol{d}_{\boldsymbol{k}}$ must be nonzero and an even function of $\boldsymbol{k}_\parallel$. The anomalous Green's function in Eq. (14) has a pairing correlation belonging to the odd-frequency symmetry class which is proportional to $\boldsymbol{\alpha}_{\boldsymbol{k}} \times \boldsymbol{d}_{\boldsymbol{k}}$. It has been established that odd-frequency Cooper pairs decrease the transition temperature and make the superconducting state unstable [26,27]. Therefore, $\boldsymbol{d}_{\boldsymbol{k}}$ should be determined self-consistently to minimize the amplitude of the odd-frequency pairing correlation and, as a result, maximize the product $\boldsymbol{\alpha}_{\boldsymbol{k}} \cdot \boldsymbol{d}_{\boldsymbol{k}}$. To reproduce the interference pattern in Fig. 2(b), $\boldsymbol{\alpha}_{\boldsymbol{k}} \cdot \boldsymbol{d}_{\boldsymbol{k}}$ must also be an odd function of k_x. The most stable state $\boldsymbol{\alpha}_{\boldsymbol{k}} \parallel \boldsymbol{d}_{\boldsymbol{k}}$, however, does not indicate such an interference pattern.

Finally, we consider the possibility of an exotic superconducting state in β-Bi_2Pd. Because of the complicated electronic structures at the Fermi level, β-Bi_2Pd may be a multiband/orbital SC [19]. The symmetry classification of order parameters in the presence of such an extra internal degree of freedom is shown in Table II [28].The momentum parity represents widely accepted symmetry options such as even-parity s wave and odd-parity p wave. When two electrons in the same conduction band form a Cooper pair, such a pair belongs to the even-band-parity class. The pairing correlation function remains unchanged (is symmetric) under the permutation of the band indices of two electrons. Therefore, conventional symmetry classes are included in the first two rows of Table II. When an electron in one band and an another electron in a different band form a Cooper pair, such a pair is called an interband pair. Interband Cooper pairs are classified into two different classes: the even-band-parity class and odd-band-parity class. The pairing correlation function of the former (latter) class is symmetric (antisymmetric) under the permutation of two band indices. The last two rows in Table II correspond to the additional symmetry classes of a multiband SC. Here we discuss how to interpret the experimental findings [18] in the presence of multiband degrees of freedom of an electron. The π-phase shift in the experiment can be explained only by odd-momentum-parity symmetry of the pair potential. The experimental results can be explained if the pair potential in β-Bi_2Pd belongs to the spin-singlet odd-momentum-parity, odd-band-parity class. At present, odd-band-parity superconductivity is only a toy model in theories [27,29]. However, the experiment [18] might indicate a signature of exotic superconductivity.

VI. CONCLUSION

We studied the effects of Rashba spin-orbit interaction on the lowest-order Josephson coupling in a spin-singlet/spin-triplet superconductor junction fabricated on a substrate. The connection between the two superconductors is described by the tunnel Hamiltonian, and the Josephson current is calculated using linear response theory. We derived selection rules for the spin and orbital parts of the pair potential in a spin-triplet SC. Based on the selection rules obtained theoretically and the interference patterns observed experimentally in a superconducting quantum interference device, we specified a possible pair potential in β-Bi_2Pd.

DATA AVAILABILITY

No data were created or analyzed in this study.

APPENDIX A: SUMMATION OVER THE WAVE NUMBER

In this Appendix, we explain how to carry out the summation over the wave number.

Within the linear response, the Josephson current between the two SCs is calculated as [23]

$$J = -2et^2 T \sum_{\omega_n} \int d\xi_s\, N_s(\xi_s) \int d\xi_t\, N_t(\xi_t)\, \mathrm{Im}\, \mathrm{Tr}\left[\left\langle \hat{F}_s(\xi_s, \Delta_{\boldsymbol{p}})\, \underset{\sim}{\hat{F}_t}(\xi_t, \boldsymbol{d}_{\boldsymbol{k}})\, \delta_{\boldsymbol{k}_\parallel, \boldsymbol{p}_\parallel} \right\rangle_{\bar{k}_\parallel}\right]. \tag{A1}$$

In a spin-singlet SC, the integral over ξ_s is carried out as

$$\begin{aligned}
&\int d\xi_s N_s(\xi_s) \frac{\xi_s^2 + \boldsymbol{\alpha}_{\boldsymbol{p}}^2 + \Omega_s^2 + 2\xi_s \boldsymbol{\alpha}_{\boldsymbol{p}} \cdot \hat{\boldsymbol{\sigma}}}{\left(\xi_s^2 + \boldsymbol{\alpha}_{\boldsymbol{p}}^2 + \Omega_s^2 + 2\xi_s|\boldsymbol{\alpha}_{\boldsymbol{p}}|\right)\left(\xi_s^2 + \boldsymbol{\alpha}_{\boldsymbol{p}}^2 + \Omega_s^2 - 2\xi_s|\boldsymbol{\alpha}_{\boldsymbol{p}}|\right)} \\
&= \int d\xi_s \left[\frac{N_s(\xi_s)}{(\xi_s - |\boldsymbol{\alpha}_{\boldsymbol{p}}|)^2 + \Omega_s^2} + \frac{N_s(\xi_s)}{(\xi_s + |\boldsymbol{\alpha}_{\boldsymbol{p}}|)^2 + \Omega_s^2} + \left(\frac{N_s(\xi_s)}{(\xi_s - |\boldsymbol{\alpha}_{\boldsymbol{p}}|)^2 + \Omega_s^2} - \frac{N_s(\xi_s)}{(\xi_s + |\boldsymbol{\alpha}_{\boldsymbol{p}}|)^2 + \Omega_s^2} \right) \frac{\boldsymbol{\alpha}_{\boldsymbol{p}} \cdot \hat{\boldsymbol{\sigma}}}{|\boldsymbol{\alpha}_{\boldsymbol{p}}|} \right] \\
&= \frac{\pi}{\Omega_s} \left[N_s(|\boldsymbol{\alpha}_{\boldsymbol{p}}|) + N_s(-|\boldsymbol{\alpha}_{\boldsymbol{p}}|) + \{N_s(|\boldsymbol{\alpha}_{\boldsymbol{p}}|) - N_s(-|\boldsymbol{\alpha}_{\boldsymbol{p}}|)\} \frac{\boldsymbol{\alpha}_{\boldsymbol{p}} \cdot \hat{\boldsymbol{\sigma}}}{|\boldsymbol{\alpha}_{\boldsymbol{p}}|} \right] \approx \frac{2\pi N_s(0)}{\Omega_s} \left[1 + X_s \frac{\boldsymbol{\alpha}_{\boldsymbol{p}} \cdot \hat{\boldsymbol{\sigma}}}{|\boldsymbol{\alpha}_{\boldsymbol{p}}|} \right],
\end{aligned} \tag{A2}$$

with $\Omega_s = \sqrt{\omega_n^2 + |\Delta_{\boldsymbol{p}}|^2}$. As a result, we obtain

$$\int d\xi_s\, N_s(\xi_s)\, \hat{F}_s(\xi_s, \Delta_{\boldsymbol{p}}) = -\frac{\pi N_s(0)}{\sqrt{\omega_n^2 + |\Delta_{\boldsymbol{p}}|^2}}\left(1 + X_s \frac{\boldsymbol{\alpha}_{\hat{\boldsymbol{p}}} \cdot \hat{\boldsymbol{\sigma}}}{|\boldsymbol{\alpha}_{\hat{\boldsymbol{p}}}|}\right)\Delta_{\boldsymbol{p}}\, e^{i\varphi_s} i\hat{\sigma}_y. \tag{A3}$$

In a spin-triplet SC, the integral over ξ_t is carried out as

$$\int d\xi_t N_t(\xi_t) \frac{(\xi_s^2 - \boldsymbol{\alpha}_{\boldsymbol{k}}^2 + \Omega_t^2)\boldsymbol{d}_{\boldsymbol{k}} \cdot \hat{\boldsymbol{\sigma}} + 2(\boldsymbol{d}_{\boldsymbol{k}} \cdot \boldsymbol{\alpha}_{\boldsymbol{k}})\boldsymbol{\alpha}_{\boldsymbol{k}} \cdot \hat{\boldsymbol{\sigma}} + 2\omega_n(\boldsymbol{\alpha}_{\boldsymbol{k}} \times \boldsymbol{d}_{\boldsymbol{k}}) \cdot \hat{\boldsymbol{\sigma}} - 2\xi_t \boldsymbol{\alpha}_{\boldsymbol{k}} \cdot \boldsymbol{d}_{\boldsymbol{k}}}{\xi_t^4 + 2\xi_t^2(\Omega_t^2 - \alpha_{\boldsymbol{k}}^2) + (\Omega_t^2 + \alpha_{\boldsymbol{k}}^2)^2 - 4|\boldsymbol{\alpha}_{\boldsymbol{k}} \times \boldsymbol{d}_{\boldsymbol{k}}|^2} \tag{A4}$$

$$\approx \frac{\pi N_t(0)}{\Omega_t}\left[\frac{\Omega_t^2 \boldsymbol{d}_{\boldsymbol{k}} \cdot \hat{\boldsymbol{\sigma}} + (\boldsymbol{d}_{\boldsymbol{k}} \cdot \boldsymbol{\alpha}_{\boldsymbol{k}})\boldsymbol{\alpha}_{\boldsymbol{k}} \cdot \hat{\boldsymbol{\sigma}} + \omega_n(\boldsymbol{\alpha}_{\boldsymbol{k}} \times \boldsymbol{d}_{\boldsymbol{k}}) \times \hat{\boldsymbol{\sigma}}}{\Omega_t^2 + \boldsymbol{\alpha}_{\boldsymbol{k}}^2} + X_t \frac{\boldsymbol{\alpha}_{\boldsymbol{k}} \cdot \boldsymbol{d}_{\boldsymbol{k}}}{|\boldsymbol{\alpha}_{\boldsymbol{k}}|}\right], \tag{A5}$$

with $\Omega_t = \sqrt{\omega_n^2 + |\boldsymbol{d}_{\boldsymbol{k}}|^2}$. Here we neglect $|\boldsymbol{\alpha}_{\boldsymbol{k}} \times \boldsymbol{d}_{\boldsymbol{k}}|^2$ in the denominator of Eq. (A4) to obtain a simple expression for the Josephson current. This approximation changes the Josephson current only quantitatively. As a result, we obtain

$$\int d\xi_t\, N_t(\xi_t)\, \hat{\underset{\sim}{F}}_t(\xi_t, \boldsymbol{d}_{\boldsymbol{k}}) = -\frac{\pi N_t(0)}{\Omega_t} i\hat{\sigma}_y\, e^{-i\varphi_t}\left[\boldsymbol{f}_t \cdot \hat{\boldsymbol{\sigma}} + X_t \frac{\boldsymbol{\alpha}_{\boldsymbol{k}} \cdot \boldsymbol{d}_{\boldsymbol{k}}^*}{|\boldsymbol{\alpha}_{\boldsymbol{k}}|}\right], \tag{A6}$$

$$\boldsymbol{f}_t = \frac{\Omega_t^2 \boldsymbol{d}_{\boldsymbol{k}}^* + (\boldsymbol{d}_{\boldsymbol{k}}^* \cdot \boldsymbol{\alpha}_{\boldsymbol{k}})\boldsymbol{\alpha}_{\boldsymbol{k}} - \omega_n(\boldsymbol{\alpha}_{\boldsymbol{k}} \times \boldsymbol{d}_{\boldsymbol{k}}^*)}{\Omega_t^2 + \boldsymbol{\alpha}_{\boldsymbol{k}}^2}. \tag{A7}$$

By substituting Eqs. (A3) and (A6) into Eq. (A1), we obtain Eq. (20).

For a junction consisting of two identical spin-singlet s-wave superconductors, the Josephson current is calculated as

$$J = -2et^2 T \sum_{\omega_n} \mathrm{Im}\,\mathrm{Tr}\, e^{i\varphi}\left[\frac{\pi N_s \Delta i\hat{\sigma}_y}{\sqrt{\omega_n^2 + \Delta^2}}\right]^2 = J_0 \frac{\Delta}{\Delta_0} \tanh\left[\frac{\Delta}{2T}\right], \quad J_0 \equiv \frac{\pi \Delta_0}{2eR_{\mathrm{N}}}. \tag{A8}$$

The results recover the Ambegaokar-Baratoff formula [24], where Δ_0 is the amplitude of the pair potential at zero temperature.

APPENDIX B: CURRENT IN TWO SQUIDS

Here we summarize an argument in Ref. [17]. The total current flowing in a SQUID in Fig. 2 is described by the summation of the two currents flowing in the two arms $J = J_L + J_R$. In Fig. 2(a), the two junctions are equivalent to each other at $\Phi = 0$. Thus, the currents are described as

$$J_L = J_{\mathrm{ST}} \sin\left(\varphi + \pi \frac{\Phi}{\Phi_0}\right), \tag{B1}$$

$$J_R = J_{\mathrm{ST}} \sin\left(\varphi - \pi \frac{\Phi}{\Phi_0}\right), \tag{B2}$$

$$\Phi_0 = \frac{\pi \hbar c}{e}, \tag{B3}$$

where $J_{\mathrm{ST}} > 0$ is the amplitude of the Josephson current in each arm. Since $J = 2J_{\mathrm{ST}} \sin\varphi \cos(\pi\Phi/\Phi_0)$, the maximum Josephson current in the SQUID in Fig. 2(a) becomes

$$|J|_{\max} = 2J_{\mathrm{ST}}\left|\cos\left(\pi \frac{\Phi}{\Phi_0}\right)\right|, \tag{B4}$$

which takes its maximum at $\Phi = 0$.

On the other hand, for the SQUID in Fig. 2(b), the sign change of the pair potential shifts the phase in the left junction by π. Thus, the two currents are described as

$$J_L = J_{\mathrm{ST}} \sin\left(\varphi + \pi + \pi \frac{\Phi}{\Phi_0}\right), \tag{B5}$$

$$J_R = J_{\mathrm{ST}} \sin\left(\varphi - \pi \frac{\Phi}{\Phi_0}\right). \tag{B6}$$

The maximum Josephson current in the SQUID in Fig. 2(b) results in

$$|J|_{\max} = 2J_{\mathrm{ST}}\left|\sin\left(\pi \frac{\Phi}{\Phi_0}\right)\right|, \tag{B7}$$

which takes its minimum at $\Phi = 0$. The difference between the interference patterns in the two SQUIDs tells us the odd-parity symmetry of the pair potential.

[1] G. R. Stewart, Z. Fisk, J. O. Willis, and J. L. Smith, Possibility of coexistence of bulk superconductivity and spin fluctuations in UPt_3, Phys. Rev. Lett. **52**, 679 (1984).

[2] H. R. Ott, H. Rudigier, Z. Fisk, and J. L. Smith, UBe_{13}: An unconventional actinide superconductor, Phys. Rev. Lett. **50**, 1595 (1983).

[3] S. S. Saxena, P. Agarwal, K. Ahilan, F. M. Grosche, R. K. W. Haselwimmer, M. J. Steiner, E. Pugh, I. R. Walker, S. R. Julian, P. Monthoux, G. G. Lonzarich, A. Huxley, I. Sheikin, D. Braithwaite, and J. Flouquet, Superconductivity on the border of itinerant-electron ferromagnetism in UGe_2, Nature (London) **406**, 587 (2000).

[4] S. Ran, C. Eckberg, Q.-P. Ding, Y. Furukawa, T. Metz, S. R. Saha, I.-L. Liu, M. Zic, H. Kim, J. Paglione, and N. P. Butch, Nearly ferromagnetic spin-triplet superconductivity, Science **365**, 684 (2019).

[5] L. Jiao, S. Howard, S. Ran, Z. Wang, J. Olivares Rodriguez, M. Sigrist, Z. Wang, N. P. Butch, and V. Madhavan, Chiral superconductivity in heavy-fermion metal UTe_2, Nature (London) **579**, 523 (2020).

[6] Y. S. Hor, A. J. Williams, J. G. Checkelsky, P. Roushan, J. Seo, Q. Xu, H. W. Zandbergen, A. Yazdani, N. P. Ong, and R. J. Cava, Superconductivity in $Cu_xBi_2Se_3$ and its implications for pairing in the undoped topological insulator, Phys. Rev. Lett. **104**, 057001 (2010).

[7] S. Sasaki, M. Kriener, K. Segawa, K. Yada, Y. Tanaka, M. Sato, and Y. Ando, Topological superconductivity in $Cu_xBi_2Se_3$, Phys. Rev. Lett. **107**, 217001 (2011).

[8] M. Sato, Nodal structure of superconductors with time-reversal invariance and Z_2 topological number, Phys. Rev. B **73**, 214502 (2006).

[9] M. Sato and S. Fujimoto, Topological phases of noncentrosymmetric superconductors: Edge states, Majorana fermions, and non-Abelian statistics, Phys. Rev. B **79**, 094504 (2009).

[10] R. M. Lutchyn, J. D. Sau, and S. Das Sarma, Majorana fermions and a topological phase transition in semiconductor-superconductor heterostructures, Phys. Rev. Lett. **105**, 077001 (2010).

[11] Y. Oreg, G. Refael, and F. von Oppen, Helical liquids and Majorana bound states in quantum wires, Phys. Rev. Lett. **105**, 177002 (2010).

[12] Y. Asano, Y. Tanaka, A. A. Golubov, and S. Kashiwaya, Conductance spectroscopy of spin-triplet superconductors, Phys. Rev. Lett. **99**, 067005 (2007).

[13] S.-P. Chiu, C. C. Tsuei, S.-S. Yeh, F.-C. Zhang, S. Kirchner, and J.-J. Lin, Observation of triplet superconductivity in $CoSi_2/TiSi_2$ heterostructures, Sci. Adv. **7**, eabg6569 (2021).

[14] Y. Asano, A. A. Golubov, Y. V. Fominov, and Y. Tanaka, Unconventional surface impedance of a normal-metal film covering a spin-triplet superconductor due to odd-frequency Cooper pairs, Phys. Rev. Lett. **107**, 087001 (2011).

[15] in *Helium Three*, edited by L. P. Pitaevskii and W. P. Halprin, Modern Problems in Condensed Matter Sciences Vol. 26 (North Holland, Amsterdam, 1990).

[16] T. Shishidou, H. G. Suh, P. M. R. Brydon, M. Weinert, and D. F. Agterberg, Topological band and superconductivity in UTe_2, Phys. Rev. B **103**, 104504 (2021).

[17] V. B. Geshkenbein, A. I. Larkin, and A. Barone, Vortices with half magnetic flux quanta in "heavy-fermion" superconductors, Phys. Rev. B **36**, 235 (1987).

[18] X. Xu, Y. Li, and C. L. Chien, Observation of odd-parity superconductivity with the Geshkenbein-Larkin-Barone composite rings, Phys. Rev. Lett. **132**, 056001 (2024).

[19] Y. Imai, F. Nabeshima, T. Yoshinaka, K. Miyatani, R. Kondo, S. Komiya, I. Tsukada, and A. Maeda, Superconductivity at 5.4 K in $\beta-Bi_2Pd$, J. Phys. Soc. Jpn. **81**, 113708 (2012).

[20] M. Sakano, K. Okawa, M. Kanou, H. Sanjo, T. Okuda, T. Sasagawa, and K. Ishizaka, Topologically protected surface states in a centrosymmetric superconductor $\beta-PdBi_2$, Nat. Commun. **6**, 8595 (2015).

[21] Y. Li, X. Xu, M.-H. Lee, M.-W. Chu, and C. L. Chien, Observation of half-quantum flux in the unconventional superconductor β-Bi_2Pd, Science **366**, 238 (2019).

[22] A. Millis, D. Rainer, and J. A. Sauls, Quasiclassical theory of superconductivity near magnetically active interfaces, Phys. Rev. B **38**, 4504 (1988).

[23] G. D. Mahan, *Many-Particle Physics* (Plenum, New York, 1990).

[24] V. Ambegaokar and A. Baratoff, Tunneling between superconductors, Phys. Rev. Lett. **10**, 486 (1963).

[25] Y. Asano, Y. Tanaka, M. Sigrist, and S. Kashiwaya, Josephson current in *s*-wave-superconductor/Sr_2RuO_4 junctions, Phys. Rev. B **67**, 184505 (2003).

[26] Y. Asano and A. Sasaki, Odd-frequency Cooper pairs in two-band superconductors and their magnetic response, Phys. Rev. B **92**, 224508 (2015).

[27] T. Sato, S. Kobayashi, and Y. Asano, Discontinuous transition to a superconducting phase, Phys. Rev. B **110**, 144503 (2024).

[28] A. M. Black-Schaffer and A. V. Balatsky, Odd-frequency superconducting pairing in multiband superconductors, Phys. Rev. B **88**, 104514 (2013).

[29] M. Gomes da Silva, F. Dinla Neto, I. Padilha, J. Ricardo de Sousa, and M. Continentino, First-order superconducting transition in the inter-band model, Phys. Lett. A **378**, 1396 (2014).